13. R. G. Thorne, C. Nicholson, *Proc. Natl. Acad. Sci. U.S.A.* **103**, 5567 (2006).
14. G. E. Hardingham, H. Bading, *Microsc. Res. Tech.* **46**, 348 (1999).
15. A. Rao, *Nat. Immunol.* **10**, 3 (2009).
16. A. L. Shifrin, A. Auricchio, Q. C. Yu, J. Wilson, S. E. Raper, *Gene Ther.* **8**, 1480 (2001).
17. M. Tewari *et al.*, *Cell* **81**, 801 (1995).
18. Y. Gavrieli, Y. Sherman, S. A. Ben-Sasson, *J. Cell Biol.* **119**, 493 (1992).
19. H. Huang, S. Delikanli, H. Zeng, D. M. Ferkey, A. Pralle, *Nat. Nanotechnol.* **5**, 602 (2010).
20. J. L. Farrant, *Biochim. Biophys. Acta* **13**, 569 (1954).
21. B. Sana, E. Johnson, K. Sheah, C. L. Poh, S. Lim, *Biointerphases* **5**, FA48 (2010).
22. K. Ziv *et al.*, *NMR Biomed.* **23**, 523 (2010).
23. B. Iordanova, C. S. Robison, E. T. Ahrens, *J. Biol. Inorg. Chem.* **15**, 957 (2010).
24. D. Halperin *et al.*, in *Proceedings of the 2008 IEEE Symposium on Security and Privacy*, Oakland, CA, 18 to 21 May 2008, pp. 129–142.
25. S. A. Hanna, paper presented at the Third International Symposium on Medical Information and Communication Technology, Montreal, Canada, 24 to 27 February 2009.
26. A. C. Nathwani *et al.*, *N. Engl. J. Med.* **365**, 2357 (2011).
27. C. A. Butts *et al.*, *Biochemistry* **47**, 12729 (2008).

Acknowledgments: We thank Friedman laboratory members for helpful discussions, S. Korres for assistance with manuscript preparation, S. Tavazoie for helpful discussions, R. Toledo-Crow and S. Abeytunge for assistance with RF technology, and the staff of the Rockefeller University Electron Microscopy Resource center for their technical support in imaging. This project was supported by funding from the JPB Foundation and grant no. R01 GM095654 from the NIH. The authors have filed a patent related to this work.

Supplementary Materials
www.sciencemag.org/cgi/content/full/336/6081/604/DC1
Materials and Methods
Supplementary Text
Figs. S1 to 10
References (*28*–*35*)

17 November 2011; accepted 23 March 2012
10.1126/science.1216753

Substrate-Controlled Succession of Marine Bacterioplankton Populations Induced by a Phytoplankton Bloom

Hanno Teeling,[1]* Bernhard M. Fuchs,[1]* Dörte Becher,[2,5] Christine Klockow,[1,3] Antje Gardebrecht,[6] Christin M. Bennke,[1] Mariette Kassabgy,[1] Sixing Huang,[1] Alexander J. Mann,[1,3] Jost Waldmann,[1,2,3] Marc Weber,[1,3] Anna Klindworth,[1,3] Andreas Otto,[5] Jana Lange,[2] Jörg Bernhardt,[5,7] Christine Reinsch,[2] Michael Hecker,[2,5] Jörg Peplies,[8] Frank D. Bockelmann,[9] Ulrich Callies,[9] Gunnar Gerdts,[4] Antje Wichels,[4] Karen H. Wiltshire,[4] Frank Oliver Glöckner,[1,3] Thomas Schweder,[2,6]† Rudolf Amann[1]†

Phytoplankton blooms characterize temperate ocean margin zones in spring. We investigated the bacterioplankton response to a diatom bloom in the North Sea and observed a dynamic succession of populations at genus-level resolution. Taxonomically distinct expressions of carbohydrate-active enzymes (transporters; in particular, TonB-dependent transporters) and phosphate acquisition strategies were found, indicating that distinct populations of *Bacteroidetes*, *Gammaproteobacteria*, and *Alphaproteobacteria* are specialized for successive decomposition of algal-derived organic matter. Our results suggest that algal substrate availability provided a series of ecological niches in which specialized populations could bloom. This reveals how planktonic species, despite their seemingly homogeneous habitat, can evade extinction by direct competition.

Annually recurring spring phytoplankton blooms with high net primary production (NPP) characterize eutrophic upwelling zones and coastal oceans in higher latitudes. Coastal zones with water depths <200 m constitute ~7% of the global ocean surface (*1*), yet they are responsible for ~19% of the oceanic NPP (*2*) and globally account for 80% of organic matter burial and 90% of sedimentary mineralization (*1*). Heterotrophic members of the picoplankton—mostly *Bacteria*—reprocess about half of the oceanic NPP in the so-called "microbial loop" (*3*). The bulk of this bacterioplankton biomass is free-living, but up to 20% is attached to algae or particles (*4*).

The bacterial response to coastal phytoplankton blooms has been almost exclusively studied in microcosm/mesocosm experiments (*5*–*8*) or with limited resolution in time and biodiversity in situ (*9*–*11*). We observed bacterial populations during and after a phytoplankton bloom in spring 2009 at the island of Helgoland in the German Bight (54°11′03″N, 7°54′00″E; fig. S1A) with a high taxonomic and functional resolution. We sampled 500 liters of subsurface seawater twice a week during 2009. Samples were filtered into fractions dominated by free-living bacteria (3 to 0.2 μm in size) and algae/particle-associated bacteria (10 to 3 μm in size) (fig. S2). Algal composition was determined microscopically (fig. S3 and table S1), and microbial composition was identified via catalyzed reporter deposition fluorescence in situ hybridization (CARD-FISH, tables S2 and S3). At selected sampling times during and after the bloom, the data were complemented by comparative analysis of 16*S* ribosomal RNA (rRNA) gene amplicons (pyrotags, table S4) and by functional data from extensive metagenome and metaproteome analyses (table S5). In addition, physical and chemical parameters were measured daily, including temperature, turbidity, salinity, and concentrations of phosphate, nitrate, nitrite, ammonium, silicate, and chlorophyll a (table S6).

Pre-bloom bacteria (Fig. 1A) were dominated by *Alphaproteobacteria* (41 to 67%), composed roughly of two-thirds SAR11 clade and one-third *Roseobacter* clade (Fig. 1B and fig. S4B). SAR11 consisted almost exclusively of subgroup Ia (*Candidatus Pelagibacter ubique*) (table S4). This composition changed as the spring phytoplankton bloom commenced (*12*). In early April (3 to 9 April 2009), *Bacteroidetes* abundances increased fivefold within 1 week (from 1.5×10^5 to 7.7×10^5 cells/ml), whereas *Alphaproteobacteria* (from 2.1×10^5 to 5.0×10^5 cells/ml) and *Gammaproteobacteria* (from 0.8×10^5 to 1.8×10^5 cells/ml) abundances only approximately doubled. The *Bacteroidetes* consisted mostly of *Flavobacteria* (89 to 98%) (table S4), with a succession of *Ulvibacter* spp., followed by *Formosa*-related and *Polaribacter* species as the most prominent groups (Fig. 1C and fig. S4C). *Gammaproteobacteria* reacted later to algal decay, but with a more dense succession of peaking clades, with highest abundances in *Reinekea* spp. and SAR92 (Fig. 1D and fig. S4D). *Reinekea* spp. grew within 1 week from 1.6×10^3 cells/ml to above 1.6×10^5 cells/ml (estimated doubling time, 25 hours) and subsequently almost vanished within 2 weeks. *Roseobacter* clade members also showed a succession, with the NAC11-7 lineage dominating the early bacterioplankton bloom and the *Roseobacter* clade–affiliated (RCA) lineage dominating the late bloom (table S4).

Metagenomes were partitioned into taxonomically coherent bins (taxobins, fig. S5A) and then used for identification, annotation, and semiquantitative analyses of the metaproteome data (*12*). This allowed the investigation of shifts in gene content and expression within dominating bacterial populations (table S7).

[1]Max Planck Institute for Marine Microbiology, Celsiusstrasse 1, 28359 Bremen, Germany. [2]Institute of Marine Biotechnology, Walther-Rathenau-Strasse 49a, 17489 Greifswald, Germany. [3]Jacobs University Bremen, Campus Ring 1, 28759 Bremen, Germany. [4]Alfred Wegener Institute for Polar and Marine Research, Biologische Anstalt Helgoland, 27483 Helgoland, Germany. [5]Institute for Microbiology, Ernst-Moritz-Arndt University, Friedrich-Ludwig-Jahn-Strasse 15, 17487 Greifswald, Germany. [6]Pharmaceutical Biotechnology, Ernst-Moritz-Arndt University, Felix-Hausdorff-Strasse 3, 17487 Greifswald, Germany. [7]DECODON, Walther-Rathenau-Strasse 49a, 17489 Greifswald, Germany. [8]Ribocon, Fahrenheitstrasse 1, 28359 Bremen, Germany. [9]HZG Research Center, Max-Planck Strasse 1, 21502 Geesthacht, Germany.

*These authors contributed equally to this work.
†To whom correspondence should be addressed. E-mail: schweder@uni-greifswald.de (T.S.); ramann@mpi-bremen.de (R.A.)

A pronounced peak in the abundance of carbohydrate-active enzymes [CAZymes (*13*)] accompanied the bacterial succession (fig. S5B). CAZyme frequencies and expressions were taxonomically distinct (Figs. 2 and 3). For instance, *Flavobacteria* and *Gammaproteobacteria* dominated the abundant glycoside hydrolase family 16 (GH16). Most corresponding genes were annotated as laminarinases for decomposing the algal glucan laminarin. Likewise, expressed GH30-family proteins that include β-D-fucosidases mapped exclusively to *Flavobacteria*. *Flavobacteria* also dominated GH29/GH95-family genes containing α-L-fucosidases, as well as L-fucose permease genes. Fucose is a major constituent of diatom exopolysaccharides (*14, 15*). *Flavobacteria* were also dominating GH92-family glycoside hydrolases encoding mainly alpha-mannosidase, whereas *Gammaproteobacteria* dominated the glycoside hydrolase family 81. Likewise, *Gammaproteobacteria* (SAR92 clade) and *Flavobacteria* dominated expression within the GH3 family.

Many algal polysaccharides are sulfated (such as carragenans, agarans, ulvans, and fucans), and hence sulfatases are required for their complete degradation. Sulfatase gene frequencies peaked together with the CAZymes at 7 April and showed a mixed taxonomic composition, but the maximum in sulfatase expression occurred later in the bloom (Fig. 3) and was dominated by *Flavobacteria*. Expressed sulfatases were found in the *Polaribacter* taxobin, which corroborates recent reports of high numbers of sulfatases in *Polaribacter* (*16*). In contrast, glycoside hydrolases for decomposing nonsulfated laminarin (GH16, GH55, and GH117) had their expression maxima earlier during the initial algal die-off phase.

Glycolytic exoenzymes initiate bacterial utilization of complex algal polysaccharides. As a result, shorter sugar oligomers and monomers become increasingly available and allow fast-growing opportunistic bacteria with a broader substrate spectrum to grow. Differences in nutritional strategies were apparent even between taxonomic classes; for example, in the expression of transport systems for nutrient uptake (Fig. 4A).

TonB-dependent transporter (TBDT) components dominated expressed transport proteins in *Flavobacteria*, whereas adenosine triphosphate (ATP)–binding cassette (ABC), tripartite ATP-independent periplasmic (TRAP), and tripartite tricarboxylate transporters (TTT) for low-molecular-weight (LMW) substrates were expressed only at low levels (Fig. 4A). TBDTs, originally thought to be restricted to complexed iron(III) (*17*) and vitamin B12 uptake, allow uptake of compounds that exceed the typical 600- to 800-dalton substrate range of normal porins (*18, 19*). Within *Bacteroidetes*, TBDTs are often colocalized with carbohydrate degradation modules (fig. S6) (*16*, *20*–*22*), and thus the substrate spectrum of these transporters may be much wider than anticipated (*23*), including oligosaccharides. TBDTs constituted no less than 13% of the expressed proteins identified during the bacterioplankton bloom at 31 March but only 7% in a non bloom sample at 11 February (fig. S7). This observation highlights the importance of TBDTs and corroborates a report of high TBDT expression in a coastal upwelling zone (*24*). In high-NPP zones, the capacity to take up oligomers as soon as they become transportable may constitute a major advantage over competitors restricted to smaller substrates.

In the *Gammaproteobacteria*, SAR92 featured a similar transporter expression profile as the *Flavobacteria*, whereas *Reinekea* spp. exhibited high expression of ABC and, to a lesser extent, TRAP transporters, indicating a different nutritional strategy with emphasis on the uptake of monomers (Fig. 4A).

Likewise, *Alphaproteobacteria* showed high expression levels of ABC and TRAP transporters and low levels of TBDTs and TTTs. This reflects the ecological strategy of the dominating SAR11. The well-studied representative *Pelagibacter ubique* HTCC 1062 thrives under oligotrophic conditions by means of high-affinity ABC and TRAP transporters and a constitutively expressed energy-producing proteorhodopsin (*25*–*27*). Our data confirmed constitutive proteorhodopsin expression and transporter components as the most abundant expressed proteins in the SAR11 clade, which corroborates previous findings (*28*). Members of the metabolically diverse, opportunistic alphaproteobacterial *Roseobacter* clade (*29*–*31*) exhibited LMW transporter expression levels that exceeded those of SAR11 (Fig. 4A). Although *Roseobacter* clade cells were two to four times less abundant than SAR11, they are larger, which may explain greater *Roseobacter* transporter expression.

Multiple factors may contribute to bacterioplankton bloom termination, such as predation by flagellate protozoa, viral lysis, and nutrient depletion. Phosphate limitation can spur algal exudate production, which might serve to promote the growth of phycosphere bacteria that remineralize and acquire phosphate more effectively (*32*); however, under phosphate limitation, algae and bacteria will compete. Phosphate dropped below the detection limit early in the phytoplankton bloom (fig. S1C), and the expression of several phosphate and phosphonate ABC-type uptake

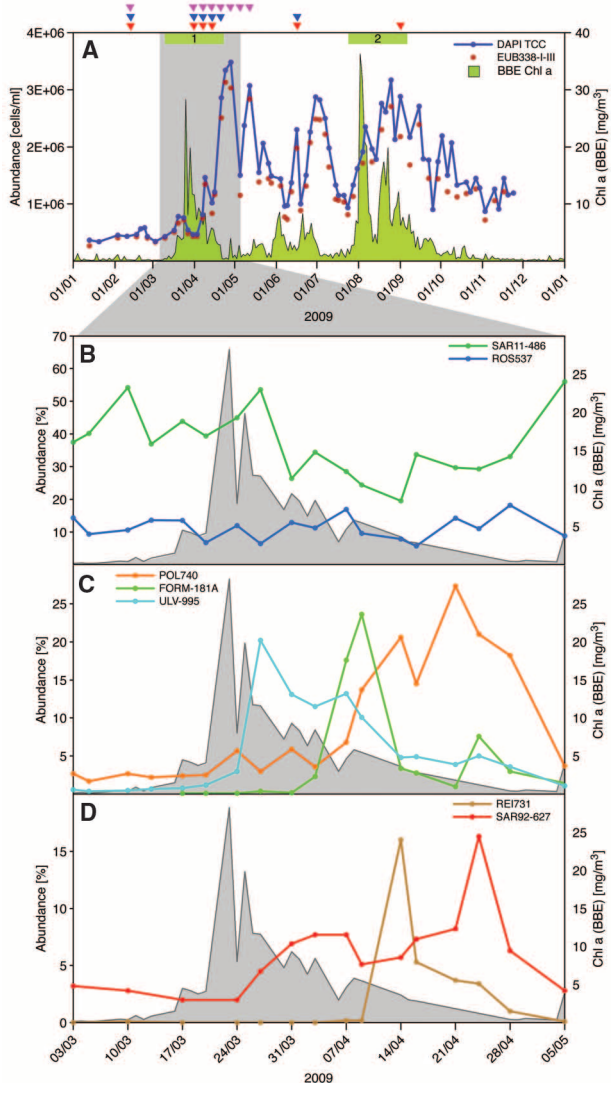

Fig. 1. Abundances of major bacterial populations during the bacterioplankton bloom as assessed by CARD-FISH. (**A**) Chlorophyll a (Chl a) concentration (measured with a BBE Moldaenke algal group analyzer), 4′,6-diamidino-2-phenylindole (DAPI)–based total cell counts (TCC), and bacterial counts (probe EUB338 I-III) during the year 2009; diatom-dominated spring blooms (1) and dinoflagellate-dominated summer blooms (2) are marked with green boxes; triangles on top mark accessory samples: metagenomics (red), metaproteomics (blue), and 16*S* rRNA gene tag sequencing (magenta). (**B**) Relative abundances of selected *Alphaproteobacteria*: SAR11 clade (probe SAR11-486) and *Roseobacter* clade (probe ROS537). (**C**) Relative abundances of selected *Flavobacteria*: *Ulvibacter* spp. (probe ULV-995), *Formosa* spp. (probe FORM-181A), and *Polaribacter* spp. (probe POL740). (**D**) Relative abundances of selected *Gammaproteobacteria*: *Reinekea* spp. (probe REI731) and SAR92 clade (probe SAR92-627). Further probes that are not shown for clarity are specified in the supplementary materials (tables S2 and S3).

Fig. 2. Abundances of CAZymes with relevance for external carbohydrate degradation. (**Left**) Copies of 20 CAZymes per megabase of metagenome sequence with class-level taxonomic classifications (*12*). Maximum abundances are highlighted in gray. (**Right**) Detailed taxonomic breakdown for four selected CAZymes showing differing taxonomic compositions; each histogram shows data for the five metagenome samples (from left to right: 11 February 2009, 31 March 2009, 7 April 2009, 14 April 2009, and 16 June 2009).

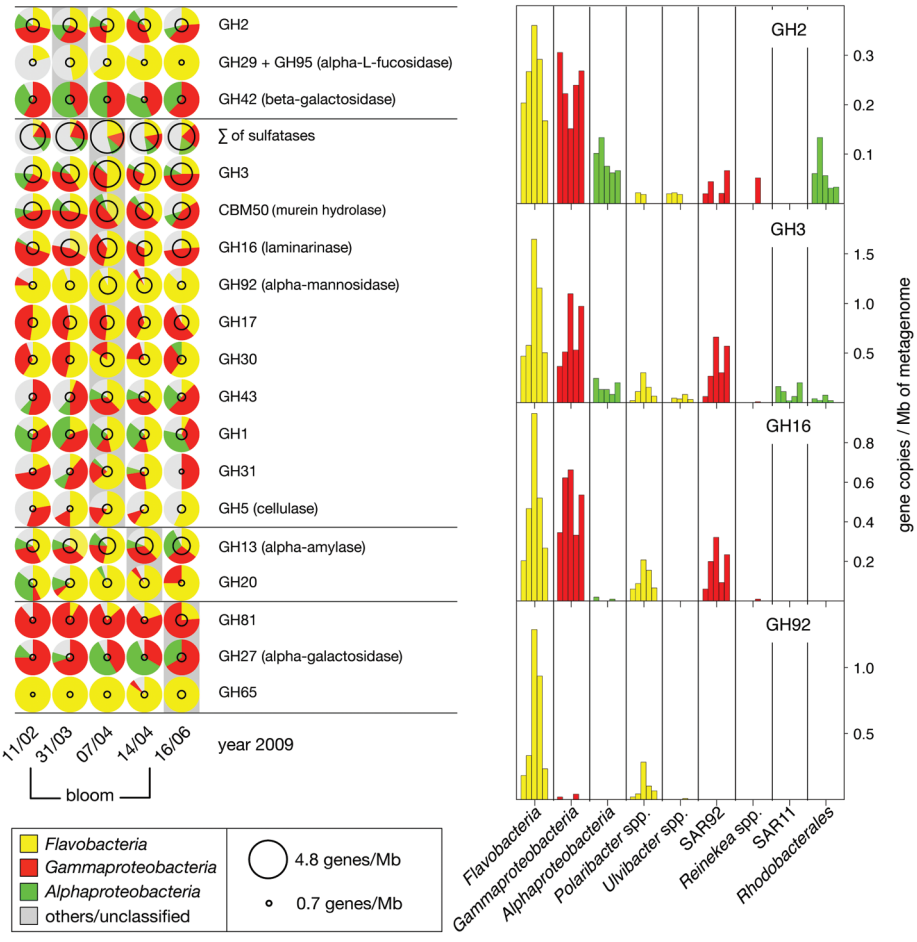

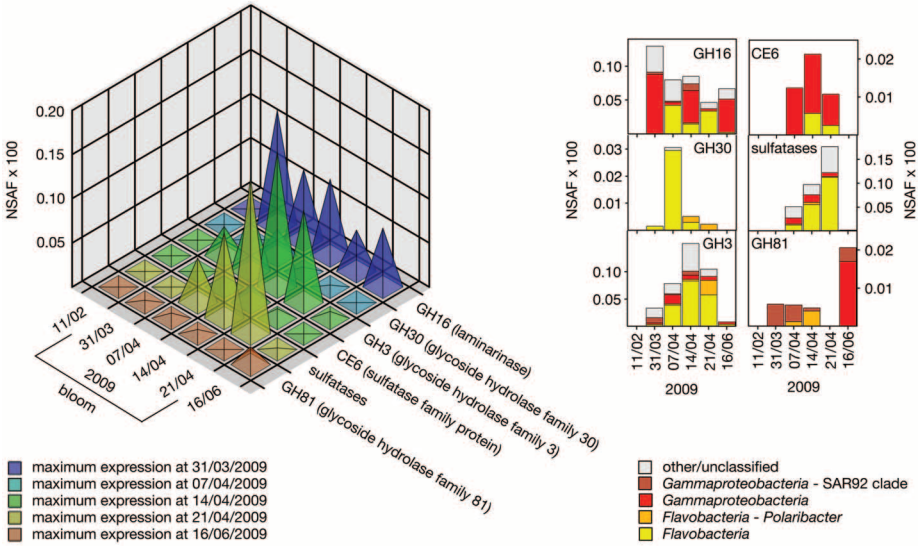

Fig. 3. Expression of CAZymes with relevance for external carbohydrate degradation; the proteome data were analyzed in a semiquantitative manner based on normalized spectral abundance factors (NSAFs) (*12*).

systems in various bacterial taxobins increased over the progression of the bloom (Fig. 4B). *Gammaproteobacteria* and SAR11 tended to use ABC-type phosphate transporters, as discovered in earlier studies (*28*), whereas flavobacterial *Polaribacter* spp. used phosphate:sodium symporters, and alphaproteobacterial *Rhodobacterales* spp. used phosphonate transporters.

In the first response to the phytoplankton bloom, flavobacterial *Ulvibacter* and *Formosa* spp. dominated (tables S2 and S4). Within these clades, TBDT components were among the proteins with the highest expression levels. This corroborates reports that specific *Flavobacteria* are tightly coupled to diatoms (*7*). *Bacteroidetes* have also been identified as major bacteria attached to marine snow (*33*, *34*), which agrees with their presumed role as fast-growing r strategists with specialization on the initial attack of highly complex organic matter (*16, 21, 35*). Hence, algal blooms lead to a multifold increase of colonization surfaces for *Bacteroidetes*, which respond with increased production of exoenzymes (*36*). After algal lysis, *Bacteroidetes* are the first to profit.

The second phase of the bacterioplankton succession coincided with a shift in algal composition (fig. S3) and was characterized by a pronounced peak of gammaproteobacterial *Reinekea* spp. that reached up to 16% of the bacteria (14 April 2009). *Reinekea* spp. featured a different expression profile, with high expression levels of transporters for peptides, phosphate, monosaccharides, and other monomers. These in situ data agree with the studies on cultured *Reinekea* species (*37*–*39*) that found broad generalist substrate spectra. The increase of alphaproteobacterial

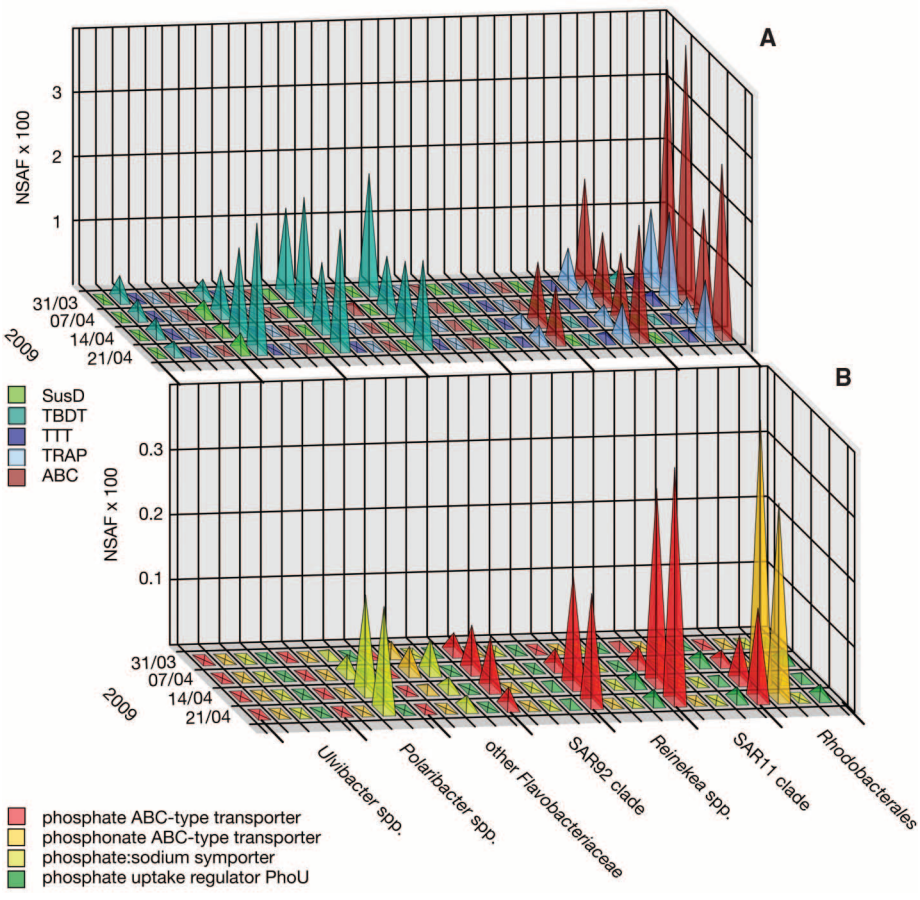

Fig. 4. Transporter components and phosphorus acquisition proteins of dominant taxa during the bacterioplankton bloom. (**A**) Expression of transporter components: starch utilization SusD-family proteins (SusD), TBDTs, TTTs, TRAPs, and ABCs. (**B**) Expression of proteins involved in phosphorus acquisition.

Roseobacter clade RCA during this phase might also be attributed to the *Roseobacter*'s opportunistic life-style (*29*) and is consistent with previous findings of free-living RCA phylotypes in the German Bight during diatom blooms (*40*).

The third phase of the spring 2009 bacterioplankton succession was dominated by flavobacterial *Polaribacter* and gammaproteobacterial SAR92 clade species, together with a secondary spike in *Formosa* spp. (Fig. 1, C and D). At this time, *Polaribacter* and *Formosa* dominated the particle/algae-attached fraction (table S8). Hence this phase with high sulfatase expression (Fig. 3) reflected another change of ecological niches (*12*).

Taken together, the bacterial response to coastal phytoplankton blooms was more dynamic than previously anticipated and consisted of a succession of distinct populations with distinct functional and transporter profiles. Thus, the diatom-induced growth of specific bacterioplankton clades most likely resulted from the successive availability of different algal primary products (bottom-up control), which provided the series of ecological niches in which specialized populations could bloom. As a result, we are now beginning to uncover the relevant predictors for defining the ecological niches of planktonic species (*41*) and thus can tackle the "paradox of the plankton" (*42*), which is how these species evade extinction by direct competition in a seemingly homogeneous habitat with limited resources.

References and Notes

1. J. P. Gattuso, M. Frankignoulle, R. Wollast, *Annu. Rev. Ecol. Syst.* **29**, 405 (1998).
2. C. B. Field, M. J. Behrenfeld, J. T. Randerson, P. Falkowski, *Science* **281**, 237 (1998).
3. F. Azam, *Science* **280**, 694 (1998).
4. F. Azam *et al.*, *Mar. Ecol. Prog. Ser.* **10**, 257 (1983).
5. J. Pinhassi *et al.*, *Aquat. Microb. Ecol.* **17**, 13 (1999).
6. L. Riemann, G. F. Steward, F. Azam, *Appl. Environ. Microbiol.* **66**, 578 (2000).
7. J. Pinhassi *et al.*, *Appl. Environ. Microbiol.* **70**, 6753 (2004).
8. J. M. Rinta-Kanto, S. Sun, S. Sharma, R. P. Kiene, M. A. Moran, *Environ. Microbiol.* **14**, 228 (2012).
9. L. B. Fandino, L. Riemann, G. F. Steward, R. A. Long, F. Azam, *Aquat. Microb. Ecol.* **23**, 119 (2001).
10. W. W. Lau, R. G. Keil, E. V. Armbrust, *Appl. Environ. Microbiol.* **73**, 2440 (2007).
11. Y. Tada *et al.*, *Appl. Environ. Microbiol.* **77**, 4055 (2011).
12. Further information is available as supplementary materials on *Science* Online.
13. B. L. Cantarel *et al.*, *Nucleic Acids Res.* **37** (Database issue), D233 (2009).
14. B. A. Wustman, M. R. Gretz, K. D. Hoagland, *Plant Physiol.* **113**, 1059 (1997).
15. V. B. Khodse, N. B. Bhosle, *Biofouling* **26**, 527 (2010).
16. P. R. Gómez-Pereira *et al.*, *Environ. Microbiol.* **14**, 52 (2012).
17. V. Braun, K. Hantke, *Curr. Opin. Chem. Biol.* **15**, 328 (2011).
18. T. K. Rostovtseva, E. M. Nestorovich, S. M. Bezrukov, *Biophys. J.* **82**, 160 (2002).
19. K. D. Krewulak, H. J. Vogel, *Biochem. Cell Biol.* **89**, 87 (2011).
20. M. Bauer *et al.*, *Environ. Microbiol.* **8**, 2201 (2006).
21. F. Thomas, J. H. Hehemann, E. Rebuffet, M. Czjzek, G. Michel, *Front. Microbiol.* **2**, 93 (2011).
22. B. M. Hopkinson, K. A. Barbeau, *Environ. Microbiol.* 10.1111/j.1462-2920.2011.02539.x (2011).
23. K. Schauer, D. A. Rodionov, H. de Reuse, *Trends Biochem. Sci.* **33**, 330 (2008).
24. R. M. Morris *et al.*, *ISME J.* **4**, 673 (2010).
25. S. J. Giovannoni *et al.*, *Science* **309**, 1242 (2005).
26. C. R. Reisch *et al.*, *Nature* **473**, 208 (2011).
27. J. Sun *et al.*, *PLoS ONE* **6**, e19870 (2011).
28. S. M. Sowell *et al.*, *ISME J.* **3**, 93 (2009).
29. M. A. Moran *et al.*, *Appl. Environ. Microbiol.* **73**, 4559 (2007).
30. T. Brinkhoff, H. A. Giebel, M. Simon, *Arch. Microbiol.* **189**, 531 (2008).
31. R. J. Newton *et al.*, *ISME J.* **4**, 784 (2010).
32. J. Tittel, O. Büttner, N. Kamjunke, *J. Plankton Res.* **34**, 102 (2012).
33. E. F. DeLong, D. G. Franks, A. L. Alldredge, *Limnol. Oceanogr.* **38**, 924 (1993).
34. D. Woebken, B. M. Fuchs, M. M. Kuypers, R. Amann, *Appl. Environ. Microbiol.* **73**, 4648 (2007).
35. J. L. Edwards *et al.*, *Genes* **1**, 371 (2010).
36. C. Arnosti, *Annu. Rev. Mar. Sci.* **3**, 401 (2011).
37. L. A. Romanenko, P. Schumann, M. Rohde, V. V. Mikhailov, E. Stackebrandt, *Int. J. Syst. Evol. Microbiol.* **54**, 669 (2004).
38. J. Pinhassi *et al.*, *Int. J. Syst. Evol. Microbiol.* **57**, 2370 (2007).
39. A. Choi, J. C. Cho, *Int. J. Syst. Evol. Microbiol.* **60**, 2813 (2010).
40. H. A. Giebel *et al.*, *ISME J.* **5**, 8 (2011).
41. S. J. Giovannoni, K. L. Vergin, *Science* **335**, 671 (2012).
42. G. E. Hutchinson, *Am. Nat.* **95**, 137 (1961).

Acknowledgments: We thank T. Hammer and T. Ferdelman for critical reading of the manuscript; M. Meiners, E. Karamehmedovic, B. Voigt, and V. Damare for sample processing; F. Ruhnau and L. Sayavedra for work on transporters; M. Zeder for automated counting; and R. Hahnke and J. Harder for help with probe testing. We are also grateful to our colleagues from the Bundesamt für Seeschifffahrt und Hydrographie for provision of operational model output. Analyses and visualizations used in fig. S1, D to F, were produced with the Giovanni online data system, developed and maintained by the NASA Goddard Earth Sciences Data and Information Service Center. We acknowledge the Moderate Resolution Imaging Spectroradiometer mission scientists and associated NASA personnel for these data. The sequence data reported in this study can be obtained from the European Bioinformatics Institute (study number ERP001227; www.ebi.ac.uk/ena/data/view/ERP001227). The German Federal Ministry of Education and Research (BMBF) supported this study by funding the Microbial Interactions in Marine Systems project (MIMAS, project 03F0480A, http://mimas-project.de).

Supplementary Materials

www.sciencemag.org/cgi/content/full/336/6081/608/DC1
Materials and Methods
Supplementary Text
Figs. S1 to S12
Tables S1 to S9
References (*43*–*102*)
Movie S1

22 December 2011; accepted 16 March 2012
10.1126/science.1218344

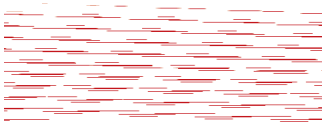

Substrate-Controlled Succession of Marine Bacterioplankton Populations Induced by a Phytoplankton Bloom

Hanno Teeling, Bernhard M. Fuchs, Dörte Becher, Christine Klockow, Antje Gardebrecht, Christin M. Bennke, Mariette Kassabgy, Sixing Huang, Alexander J. Mann, Jost Waldmann, Marc Weber, Anna Klindworth, Andreas Otto, Jana Lange, Jörg Bernhardt, Christine Reinsch, Michael Hecker, Jörg Peplies, Frank D. Bockelmann, Ulrich Callies, Gunnar Gerdts, Antje Wichels, Karen H. Wiltshire, Frank Oliver Glöckner, Thomas Schweder and Rudolf Amann (May 3, 2012)

Science **336** (6081), 608-611. [doi: 10.1126/science.1218344]

Editor's Summary

Blooming Succession

Algal blooms in the ocean will trigger a succession of microbial predators and scavengers. **Teeling *et al.*** (p. 608) used a combination of microscopy, metagenomics, and metaproteomics to analyze samples from a North Sea diatom bloom over time. Distinct steps of polysaccharide degradation and carbohydrate uptake could be assigned to clades of Flavobacteria and Gammaproteobacteria, which differ profoundly in their transporter profiles and their uptake systems for phosphorus. The phytoplankton/bacterioplankton coupling in coastal marine systems is of crucial importance for global carbon cycling. Bacterioplankton clade succession following phytoplankton blooms may be predictable enough that it can be included in models of global carbon cycling.

Science (print ISSN 0036-8075; online ISSN 1095-9203) is published weekly, except the last week in December, by the American Association for the Advancement of Science, 1200 New York Avenue NW, Washington, DC 20005.